Journal of the European Ceramic Society **10** (1992) 291–298

Phase Transformation and Microstructure of a Dense Zircon–Zirconia Composite

Wen-Cheng J. Wei

Institute of Materials Science and Engineering, National Taiwan University, Taipei, Taiwan 10764, Republic of China

&

Richard Adams

Ceramics Process Systems Corporation, Milford, Massachusetts 10757, USA

(Received 4 December 1991; revised version received 3 January 1992; accepted 28 February 1992)

Abstract

Dissociated zircon mixed with 10 wt% monoclinic zirconia was densified above the liquid-phase formation temperature (≥1676°C) to greater than 97% theoretical density. The dense material was then heat treated between 1450 and 1650°C to increase zircon-phase content through the association reaction of amorphous silica with zirconia. Optical microscopy, SEM, TEM and quantitative XRD were used to study pore evolution due to the association reaction and to measure the degree of zircon-phase formation. The reaction of amorphous silica and zirconia has reaction kinetics that can be represented as a transformation–temperature–time (TTT) diagram. The diagram yields transformation curves in a 'C' shape which imply a nucleation and growth mechanism for the reaction with a maximum reaction rate near 1600°C. Pore volume was dependent on the extent of zircon association, and homogeneously distributed in the matrix. However, below 1500°C, an interface development influenced the transformation and gave a morphology with pore cluster near mm in size. Maximum open-pore volume was 10% after heat treatment at 1550°C for 4 h.

Eine Mischung aus dissoziiertem Zirkon und 10 Gew.% monoklinem Zirkondioxid-Zusatz wurde oberhalb der Bildungstemperatur der flüssigen Phase (≥1676 C) zu einer Dichte oberhalb 97% der theoretischen Dichte verdichtet. Das verdichtete Material wurde anschließend bei Temperaturen zwischen 1450 und 1650°C wärmebehandelt, um den Anteil an Zirkonium-Phase über die Assoziationsreaktion von amorphem Siliziumdioxid mit Zirkoniumdioxid zu erhöhen. Um die Entwicklung der Porosität aufgrund der Assoziationsreaktion zu untersuchen und um den Grad der Bildung von Zirkonium-Phase zu bestimmen, wurden Lichtmikroskopie, REM, TEM und quantitative XRD eingesetzt. Die Reaktion zwischen amorphem Siliziumdioxid und Zirkoniumdioxid zeigt eine Reaktionskinetik, die in der Form eines Zeit–Temperatur–Umwandlungsdiagramms (ZTU) dargestellt werden kann. Diese Auftragung führt zu C-förmigen Umwandlungskurven. Damit können Keimbildungs- und Keimwachstumsmechanismen für die Reaktion impliziert werden. Die maximale Reaktionsrate liegt bei 1600°C. Das Porenvolumen war gleichmäßig über die Matrix verteilt und ist abhängig von dem Ausmaß der Zirkonium-Assoziation. Unterhalb 1500°C beeinflußte jedoch die Ausbildung der Grenzflächen die Umwandlung und führte zu einer Morphologie mit Poren-Clustern im mm-Größenordhung. Das maximale Volumen offener Porosität einer Wärmebehandlung von 4 h bei 1500°C entsprach 10%.

Du zircon ($ZrSiO_4$) dissocié mélangé avec 10% en masse de zircone monoclinique a été densifié à plus de 97% de la densité théorique au dessus de la température de formation de la phase liquide (≥1676°C). Le matériau dense a été par la suite traité thermiquement entre 1450 et 1650°C pour augmenter la teneur en zircon par la réaction entre de la silice amorphe et la zircone. On a utilisé la microscopie optique, le MEB, le MET et l'analyse quantitative par diffraction de RX pour étudier l'évolution des pores due à la réaction et pour mesurer le degré de formation

Journal of the European Ceramic Society 0955-2219/92/$5.00

du zircon. La réaction entre la silice amorphe et la zircone a une cinétique de réaction qui peut être représentée par un diagramme transformation–température–temps (TTT). Le diagramme présente des courbes de transformation en forme de C, ce qui implique une nucléation et un mécanisme de croissance pour la réaction, avec une vitesse maximale de réaction vers 1600°C. Le volume des pores était dépendant du degré d'association et présentait une distribution homogène dans la matrice. De plus en dessous de 1500°C, le développement d'une interface a influencé la transformation et a donné une morphologie avec des regroupements de pores d'une taille proche du mm. Le volume maximum de porosité ouverte a été de 10% pour un traitement thermique à 1550°C pendant 4 h.

1 Introduction

Zircon, a naturally occurring and inexpensive raw material, has a relatively high dissociation temperature and purity. The traditional applications of zircon are in the foundry and the refractory, which have been in use since the early twentieth century. Recently, the use of dense zircon as a refractory in continuous steel casting processes has been reported;[1,2] the material has been extensively evaluated in the past few years. Properly densified zircon composites (ZZ) can be used as tundish nozzles,[2] break rings, or in other high-temperature applications[3–7] for long-term service. The ZZ composites doped with excess zirconia have demonstrated good corrosion resistance against molten steel[1] and good thermal shock resistance,[3] and have retained high strength after thermal cycles.[2] Such high-temperature properties are attractive for the continuous casting of molten steel and for other severe conditions.

The phase diagram of the SiO_2 and ZrO_2 binary system[8] shows only zircon as an intermediate phase. The eutectic liquid comprising approximately 5% ZrO_2 and 95% SiO_2 solidifies at 1687°C and forms pure ZrO_2 (m-phase) and SiO_2 (amorphous phase). Below 1676°C, m-ZrO_2 and amorphous SiO_2 tend to react to form the stable zircon phase.[9] The association reaction

$$ZrO_2 + SiO_2 \rightarrow ZrSiO_4 \quad (1)$$

results in 19% volume shrinkage, thus producing porosity. The formation of zircon occurs in association with a volume contraction. It is likely that the phase reactions in the zircon–zirconia system generate pores and structural inhomogeneity, such as residual glassy phase.

Pure zircon powder is difficult to sinter to high density. Additives are often used to aid in densification.[10] An alternative raw material with better sinterability is dissociated zircon.[11] This material is fabricated in a plasma process[9] and consists of m-ZrO_2 and amorphous SiO_2. However, the above-mentioned dissociated powder can be easily densified above 1450°C,[4,5] when it tends to form zircon phase at the sintering temperature, consequently creating 10 vol.% or more of porosity in the densified matrix.

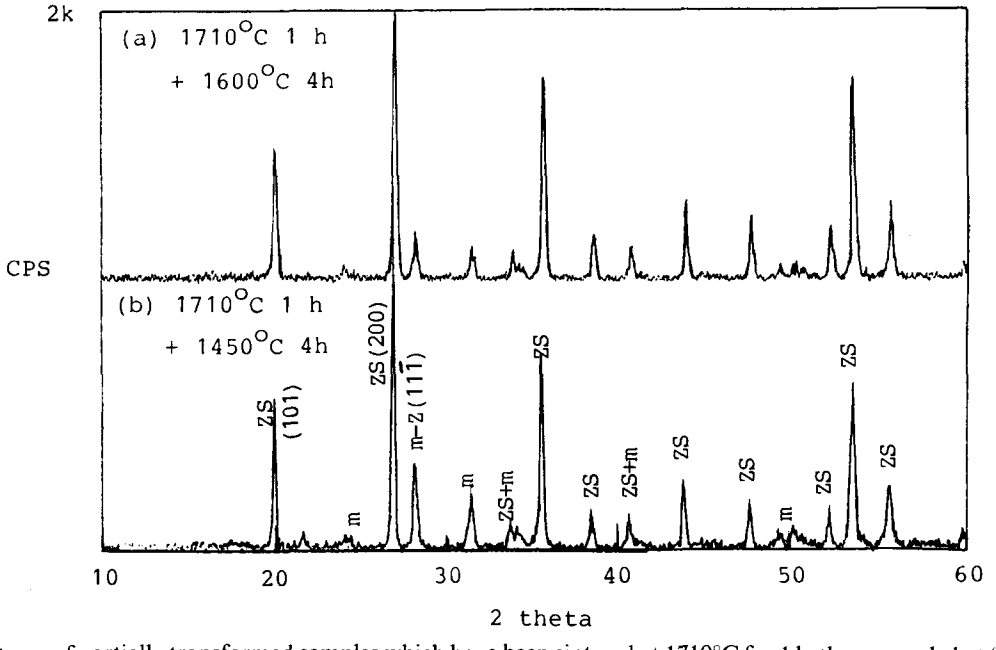

Fig. 1. XRD patterns of partially transformed samples which have been sintered at 1710°C for 1 h, then annealed at (a) 1600°C for 4 h or (b) 1450°C for 4 h.

Garvie[1,5] showed that zircon with 10 wt% of a coarse grain monoclinic ZrO_2 (m-ZrO_2) had better retained strength after thermal shock than a pure or 20% ZrO_2-doped zircon. It was reported that the additional m-ZrO_2 was responsible for the strengthening of ZZ refractories by a microcracking mechanism.

This study used a similar composition to that described by Garvie[1] and Adams & Zetz[2] to prepare a dense zircon–silica–zirconia composite, then to investigate the zircon association reaction, pore formation and its reaction kinetics. It reveals an alternative sintering route to produce dense ZZ refractories with controlled porosity.

2 Experimental

2.1 Sample preparation

Studies were based on a raw material formulation of dissociated zircon (DZ) and 10 wt% m-ZrO_2.[5] The as-received DZ powder (DS10) with impurities TiO_2 0·08%, Al_2O_3 0·36%, Fe_2O_3 0·03% and free silica 0·11% was supplied by Z-TECH Corp., Bow, NH

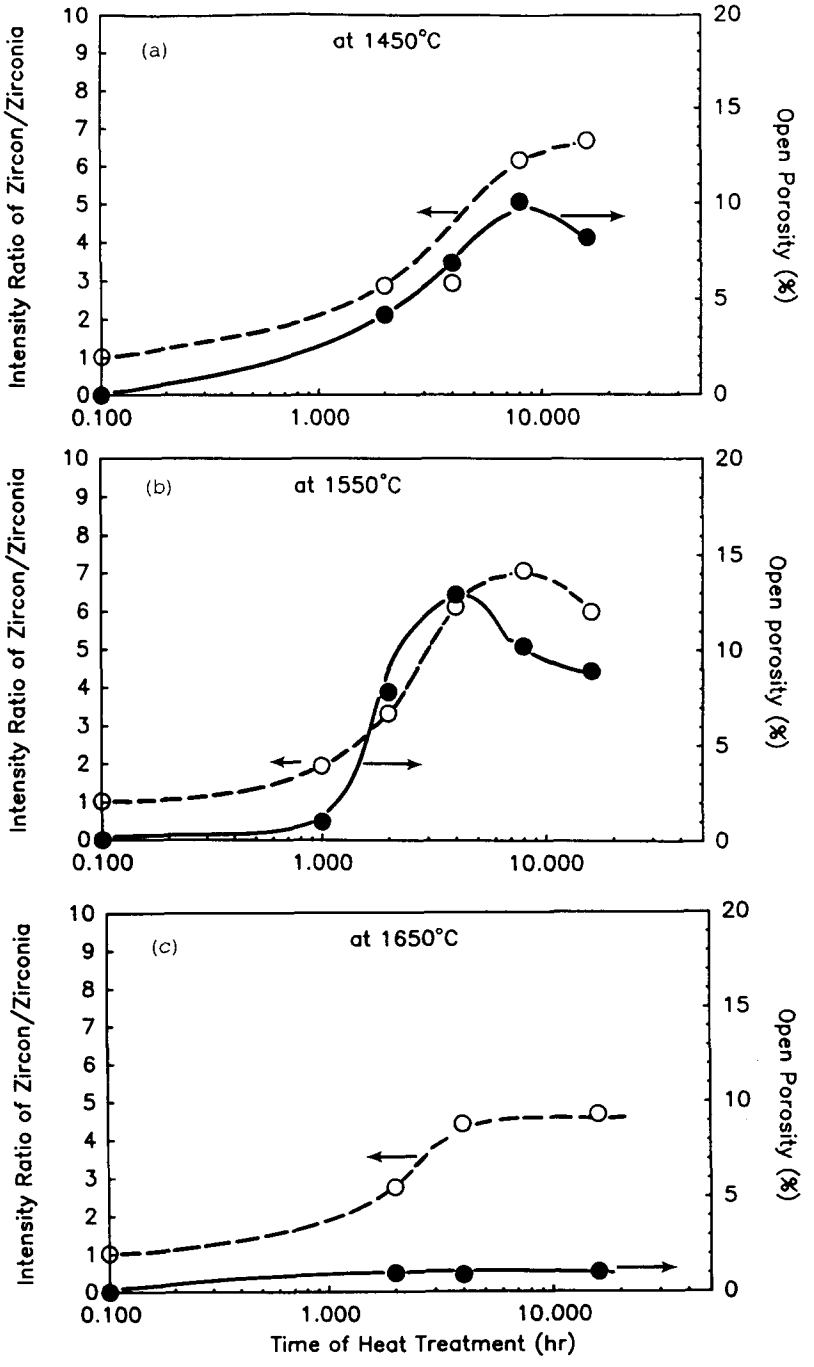

Fig. 2. X-Ray intensity ratio of zircon–zirconia phases and open porosity of the ZZ(10) samples at various times of heat treatment: (a) 1450°C; (b) 1550°C; (c) 1650°C.

03301, USA. It had an average particle size of 110 microns. This material was comminuted in an aqueous suspension with MgO-PSZ grinding media. The final average size of ground DZ powder was controlled to between 2 and 4 microns, with the coarse end of the size distribution being less than 10 micrometers. The comminuted DZ powder was mixed with 10 wt% m-ZrO_2 powder (supplied by Magnesium Elektron, Flemington, NJ, USA, MEI S-Grade (unstabilized), surface area 2–4 m^2/g, average size 3 to 4 microns with agglomerates 5 to 50 microns) in an aqueous slurry; 25 mm diameter × 5 mm thickness specimens were prepared by slip casting.

The green pieces, designated as ZZ(10), were initially densified in an air furnace at 1710°C for 1 h. This temperature promoted liquid-phase densification. The total porosity of the sintered piece was determined to be less than 1% by the Archimedes method and microscopic inspection.

The as-fired ZZ(10) samples were heat treated to promote the reaction of SiO_2 and ZrO_2 to form the zircon phase. Heat treatment temperatures ranged from 1440 to 1650°C.

2.2 Quantitative X-ray diffraction (QXRD)

Crystalline phases, zircon and m-ZrO_2, show (200) and (11$\bar{1}$) diffraction peaks, respectively, which were used to quantify the phases. Calibration standards were prepared from zircon, m-ZrO_2 and amorphous SiO_2 to convert peak X-ray intensity ratio to a weight ratio. The preparation procedures of standard samples[12] and the calculation of the conversion table have been reported elsewhere.[13]

2.3 Microscopic analysis

Polished samples were prepared by standard ceramographic procedures for optical and SEM observation. Thin foils of ZZ(10) (3 mm diameter) were prepared for TEM observation. Traditional TEM techniques such as bright field (BF), centered dark field (CDF) and selected electron diffraction (SED) were used to provide crystallographic information.

3 Results and Discussion

The as-received DS powder contained a small fraction of crystalline zircon phase. Sintering the ZZ(10) composite to 1710°C and subsequent cooling increased the zircon phase to 33 wt%. Figure 1 shows the XRD patterns of two samples which have been sintered at 1710°C for 1 h, then heat treated for

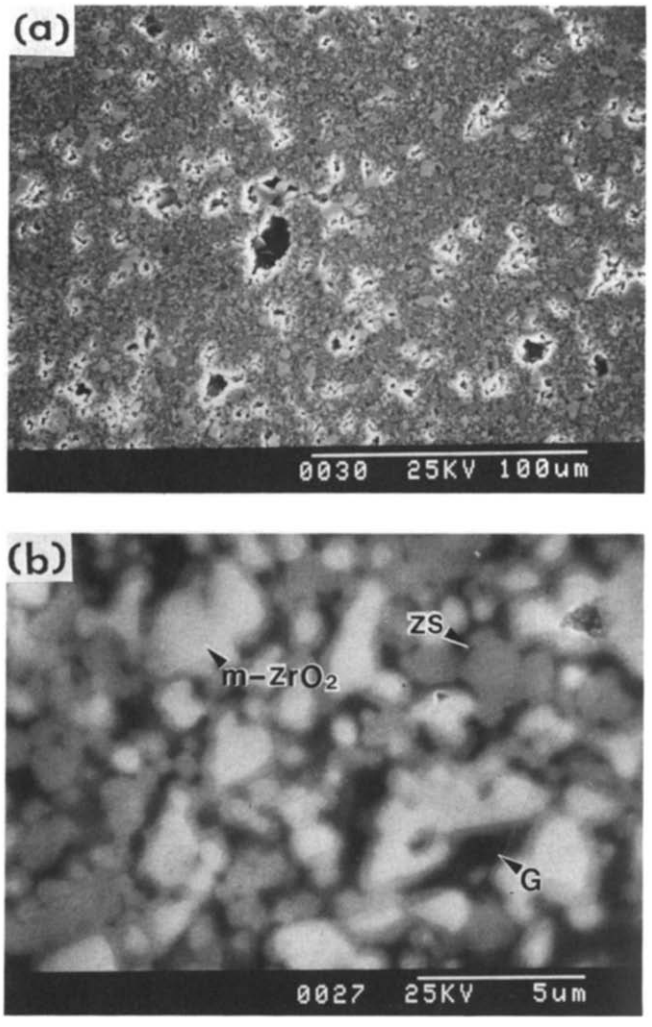

Fig. 3. SEM micrographs of ZZ(10) sample: (a) a typical microstructure of a sample densified at 1710°C for 1 h with 3 vol.% residual porosity; (b) three-phase microstructure consists of m-ZrO_2 (white), zircon (grey) and SiO_2 (black) after 1·5 h annealing at 1500°C.

4 h, one at 1600°C, the other at 1450°C. Comparison of the peak intensity ratio of zircon (200) and m-zirconia (11$\bar{1}$) reveals increased zircon content in the 1600°C sample. No tetragonal zirconia (t-ZrO_2) was detected. This is similar to the observation by McPherson *et al.*[11] that small t-ZrO_2 grains *c.* 0·2 μm or less can only be found in the sintered zircon matrix by high resolution TEM.

The X-ray intensity ratio and open porosity of ZZ samples are plotted as a function of time at the heat treatment temperatures 1450, 1550 and 1650°C in Fig. 2. The results show relatively similar quantities of zircon formation at 1450 and 1550°C, and less at 1650°C. Open porosity increases similarly at both 1450 and 1550°C, and corresponds with zircon formation. The 1650°C heat treatment does not show a similar porosity increase; apparently fine pores are eliminated by densification concurrent with zircon association. A reduction in porosity is

revealed in the lower temperature heat treatments, but after 8 to 10 h.

Figure 3(a) is a SEM micrograph of a polished ZZ(10) sample. The densified sample in general has a bimodal distribution of pore size; one of approximately 20 microns, the other is one micrometer or less. At higher magnification the SEM micrograph (Fig. 3(b)) reveals a three-phase microstructure consisting of m-ZrO_2 (white contrast), zircon (grey contrast) and SiO_2 (dark contrast). Also apparent in Fig. 3(b) are white zirconia grains surrounded by a relatively uniform thickness layer of the grey zircon phase. The SEM image contrast allows quantitative phase analysis by a quantitative ceramographic method, and can be compared with the values obtained from QXRD. Several SEM micrographs were analyzed. The results showed only $\pm 2\%$ difference to that from QXRD.

The association kinetics are represented in a TTT (transformation–temperature–time) diagram (Fig. 4) in which the amount of transformation was estimated and converted from the intensity curves for zircon/zirconia. Here the formation kinetics of the zircon phase are shown as curves from 40% to 70% of complete zircon association (the densified ZZ matrix has 33% zircon phase before heat treatment; therefore, the TTT contour line starts from 40%). The nose of the TTT curves for the reaction is at 1600°C; this is the temperature of maximum zircon association reaction rate. In addition, the shape of the TTT curves is an approximate 'C' shape, implying that nucleation and growth of the zircon phase occurred in the ZZ matrix. Such a formation mechanism of zircon phase is consistent with the TEM and optical observations.

TEM micrographs of an area similar to that in Fig. 3(b) are shown in Fig. 5. The bright field (BF) image illustrates a zircon (ZS) grain, approximately 2 micrometers in size, and surrounded by a glassy layer (G). The large grain was imaged containing dislocations and low-angle boundaries. Some of the 'grains' have a core of m-ZrO_2. This core represents an intermediate stage of the association reaction. The glassy phase, illuminated in the centered dark field (CDF) condition (Fig. 5(b)), entirely wets the ZS grain boundaries.

One of the partially reacted zircon-ZrO_2 'grains' shown in Fig. 5(a) was further examined. One BF and two CDF micrographs are shown in Fig. 6. The center grain in these micrographs is ZrO_2, surrounded with at least four zircon grains. No porosity is resolved within the grain or at the interface between zircon and the outer silicate glass phase. Zircon grains 'a' and 'c' are in bright contrast when illuminated from 101 (Fig. 6(b)) and 112 (Fig. 6(c)) diffraction intensities, respectively. This reveals that the two grains, a and c, hold different crystalline orientations and may have grown from different zircon embryos.

Microstructural modifications, including the porosity generation and the formation of zircon phase, proceed in association with the reaction of

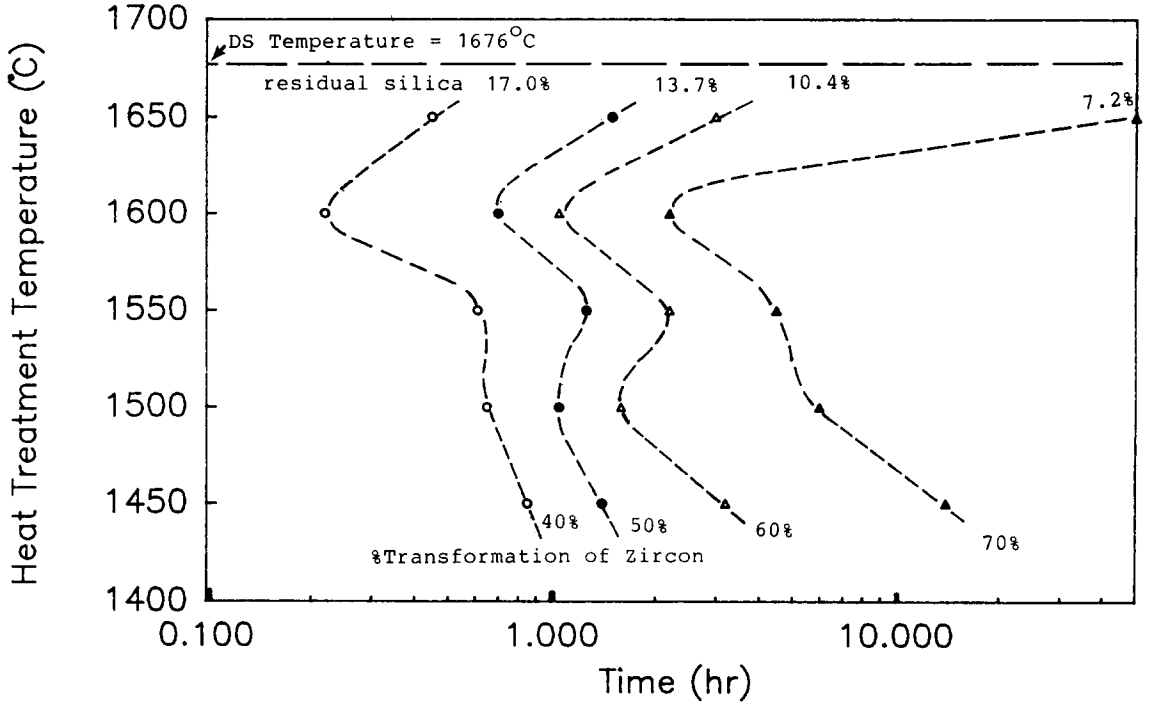

Fig. 4. Transformation–temperature–time diagram depicts the formation kinetics of zircon phase with 40 to 70 wt% transformation at a temperature below the dissociation temperature, 1676°C.

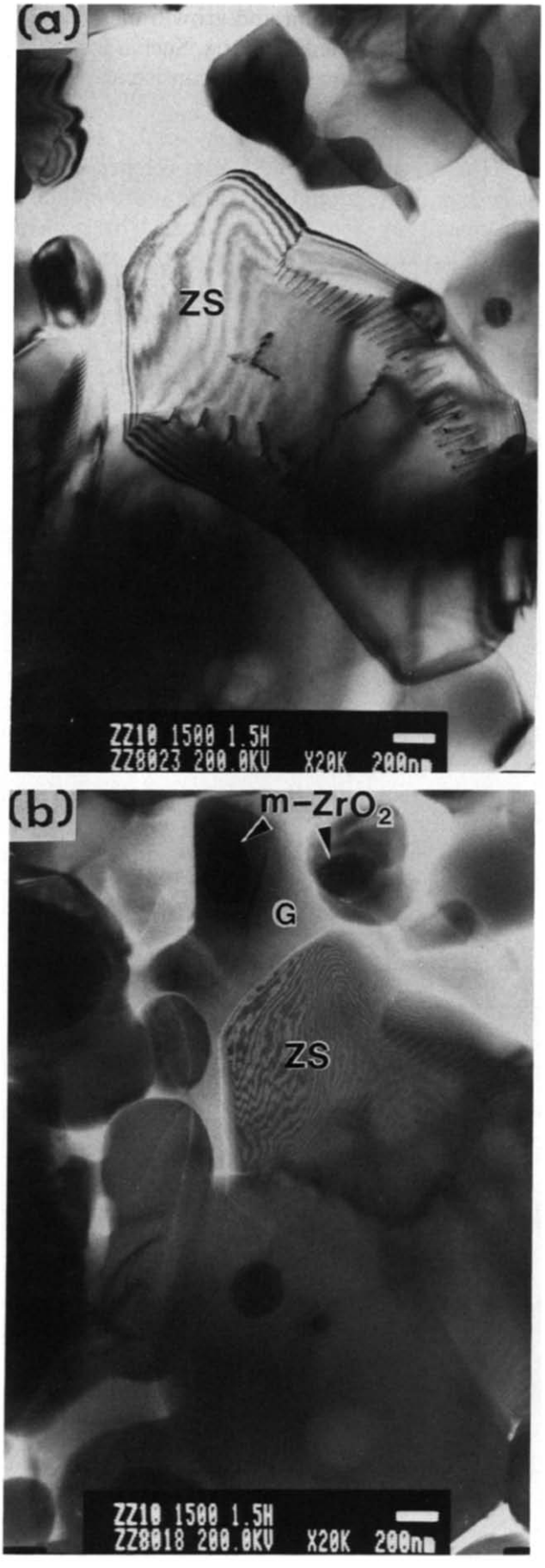

Fig. 5. TEM (a) BF and (b) CDF micrographs illustrate the dense ZZ(10) sample annealed at 1500°C for 1·5 h.

SiO_2 and ZrO_2. The association reaction should involve the outward diffusion of Zr species from a zirconia grain and the inward diffusion of Si species. The generated pores balance the volume change resulting from the above-mentioned counter-diffusion. Pores produced from the volume change associated with zircon association can coalesce in the glassy phase to form submicron porosity. The pores on the polished surface, as observed by SEM, often in micrometer size, segregate in clusters, as indicated in Fig. 7(a). These pore clusters were observed very often on the interior of the ZZ(10) samples which were heat treated below 1550°C. This suggests preferential growth of localized regions of zircon association. From the evidence of clustering of the product phase, the amount of zircon phase may be enhanced by the movement of the zircon/glass interface (as indicated on Fig. 7(b)).

The pore cluster bracketed in Fig. 7(a) is shown at higher magnification in Fig. 7(b). Regions to the left and right of Fig. 7(b) were further explored in the SEM micrographs of Fig. 8. The region of fine porosity (Fig. 8(a)) reveals a matrix with minimal free silicate glass. The microstructure is composed mostly of zircon and a few zirconia grains. The region which appears in Fig. 7(b) as a denser region is shown in the SEM micrograph of Fig. 8(b). This region has a distinctly different microstructure from the more porous region; higher levels of both glass and zirconia are clearly evident.

As the TTT curves imply, the formation of zircon grains in the ZZ(10) matrix can be controlled by a nucleation and growth mechanism. The evidence is depicted in Figs 6 and 7. The fastest rate of zircon formation is near 1600°C. The diffusion of Zr and Si species and the stability of zircon phase have a reverse temperature dependence. As a result, the formation of zircon is a multiple of the above-mentioned nucleation and growth factors. The combined effect of these two factors gives a C-shape transformation curve: a fast rate near 1600°C and lower rates at either $\geq$1600 or $\leq$1550°C.

The phase formation can start either from heterogeneous nucleation on residual zircon or from the formation of zircon embryos at the interface of ZrO_2/silicate. It is suggested from Fig. 7 that heterogeneous nucleation is dominating, especially in the temperature region below 1550°C, because of the abundant residual zircon grains (33 wt%) in the as-sintered ZZ(10) specimen. The zircon formation could be locally enhanced by the movement of the interface reaction, and the ZZ(10) matrix could undergo different degrees of pore cluster formation in different regions.

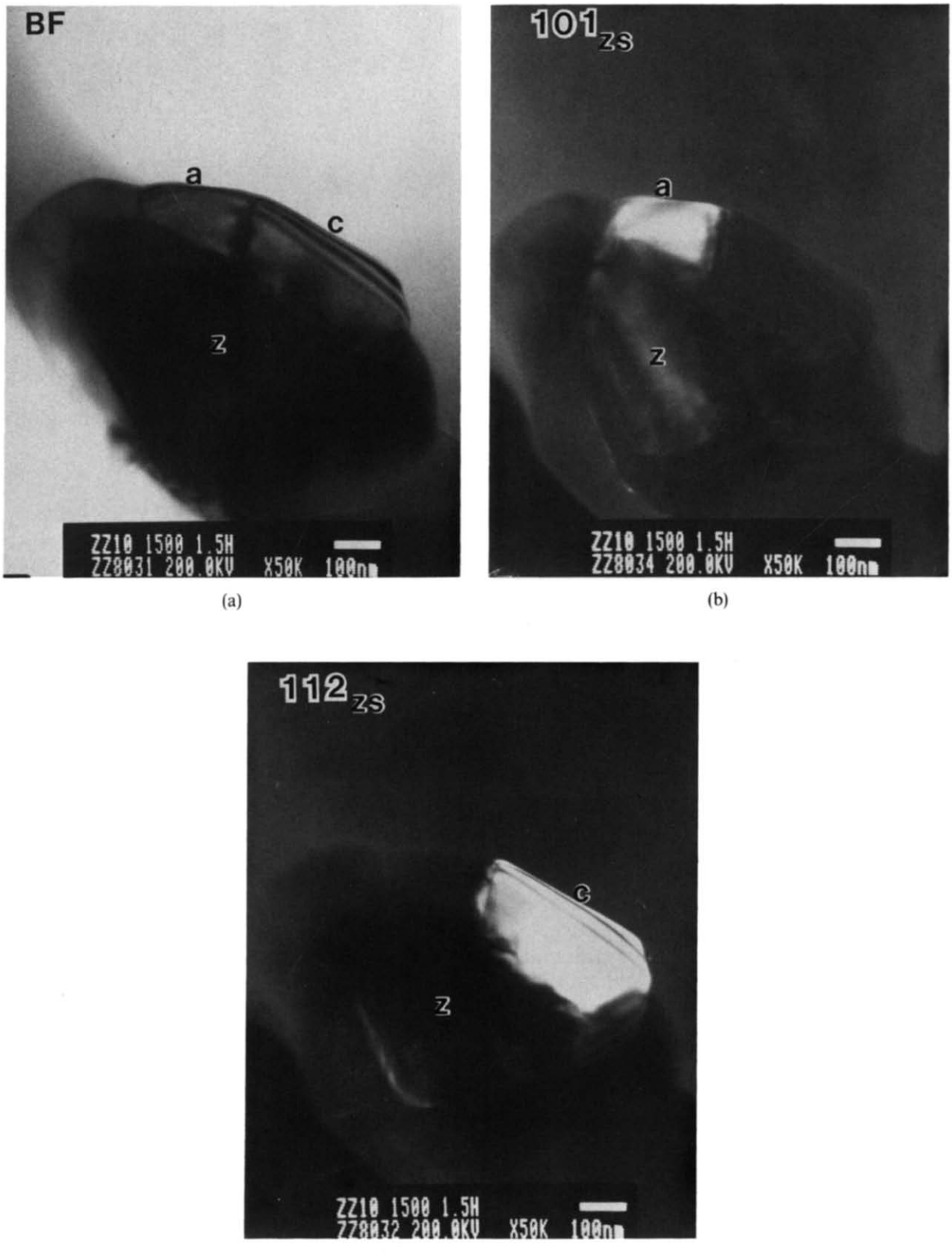

(a) (b) (c)

Fig. 6. TEM micrographs of the sample in Fig. 5 showing the newly formed zircon ('a' or 'c' grain) surrounding a m-ZrO_2 grain ('z') and with polycrystalline character: (a) BF image; (b) and (c) CDF micrographs imaged with the selected diffraction intensity.

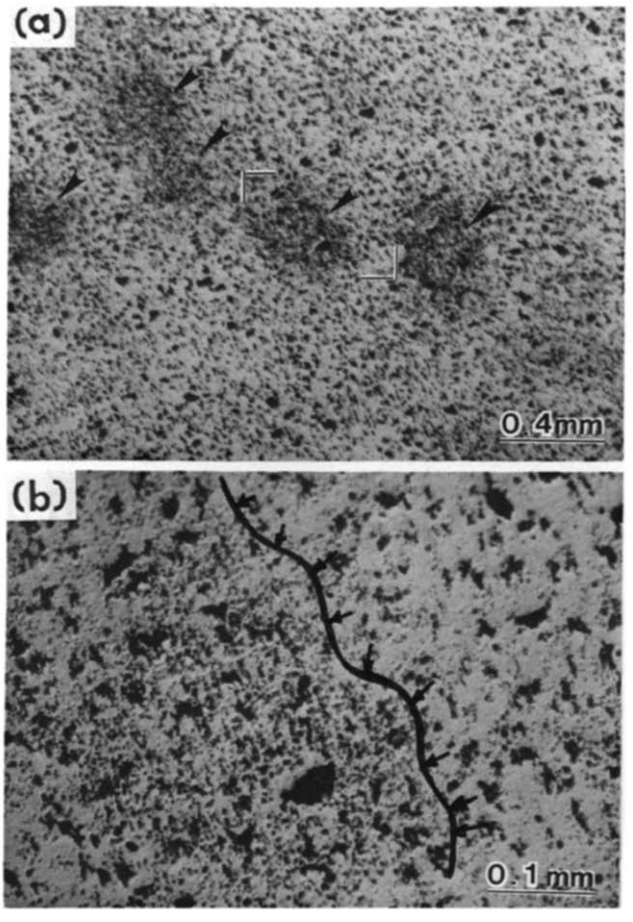

Fig. 7. Optical micrographs of polished ZZ(10) sample densified at 1710°C for 1 h and annealed at 1450°C for 4 h: (a) porosity clusters, as-pointed, imaged by a side illumination; (b) magnified centered region in (a) showing the fine porous region (left half) in contrast to the partially transformed region (right half).

4 Conclusion

A dissociated zircon with 10 wt% ZrO_2 composition densified above the eutectic temperature to produce a matrix composed of 33·5 wt% zircon, 19 wt% SiO_2 and 47·5 wt% m-ZrO_2. Heat treatment at temperatures from 1450 to 1650°C results in increased zircon content due to the reaction of SiO_2 and ZrO_2. The volume change associated with the reaction transformation produces a substantial amount of porosity, which can increase from 1 vol.% in as-fired parts to more than 10 vol.% in heat-treated parts. Heat treatment, therefore, alters the relative phase content of SiO_2, ZrO_2 and zircon, and the volume and size distribution of porosity. The formation kinetics of the zircon phase can be represented in a TTT diagram and show a maximum rate at 1600°C. The kinetics seem to follow a heterogeneous nucleation and growth mechanism. At lower temperature ($\leq$1500°C), interface movement during the formation of the zircon phase gives a clustering morphology of pores. Heat treatment at 1650°C resulted in increased zircon content but minimal increase in porosity, presumably due to concurrent additional densification.

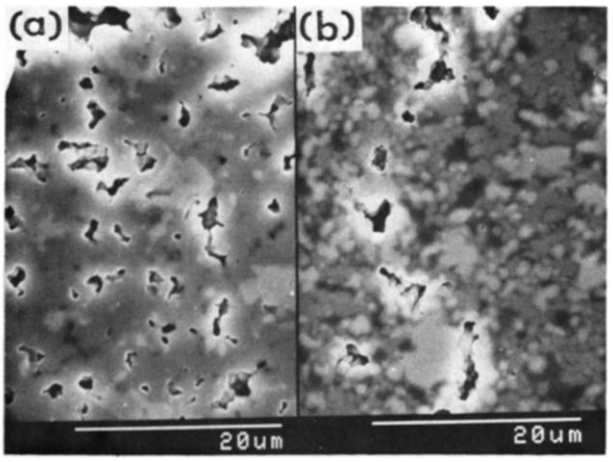

Fig. 8. SEM micrographs illustrate the regions mentioned in Fig. 7(b): (a) fine porous region has nearly transformed to zircon with some ZrO_2 grains left; (b) partially transformed to zircon, with the evidence of residual silicate glass (dark contrast).

References

1. Garvie, R. C., Improved thermal shock resistant refractories from plasma dissociated zircon. *J. Mat. Sci.*, **14** (1979) 817–22.
2. Adams, R. & Zetz, M., Performance and analysis of fine grained, high density ceramics used as tundish nozzles for continuous casting of steel. In *Proc. Unified Int. Tech. Conf. on Refract.*, ed. L. J. Forster. First Biannual Worldwide Conf on Refract., Anaheim, CA, 1–4 November 1989, pp. 635–44.
3. Adams, R. W. & Wei, W. J., Refractory ceramics for contact with molten metal. US Patent 4 888 313, 19 December 1989.
4. Williamson, J. P. H. & Morriss, H. A., Production of refractory articles. US Patent 4 053 320, 11 October 1977.
5. Garvie, R. C., Zircon/zirconia refractories. US Patent 4 579 829, 1 April 1986.
6. Toshiba Ceramics, Zircon–zirconia refractory for glass furnace lining—prepared by using isostatic pressing machine and calcination. Japanese Patent 7 635 473, 3 October 1977.
7. Kurosaki Refractory, Zircon and/or zirconia bases refractory is made from raw materials containing controlled amount of particles not more than 10 microns in size. Japanese Patent 8 389 391, May 1983.
8. Phase diagram, No. 2400, in the 'Phase Diagram for Ceramics', Vol. II, Am. Ceram. Soc., Ohio, USA, 1969.
9. Evans, A. M. & Williamson, J. P. H., Composites and microstructure of dissociated zircon produced in a plasma furnace. *J. Mat. Sci.*, **12** (1970) 779–90.
10. Rogers, M. G., Zircon-containing composites and ceramic bodies formed from such composition. US Patent 4 152 166, 1 May 1979.
11. McPherson, R., Shafer, B. V. & Wong, A. M., Zircon–zirconia ceramics prepared from plasma dissociated zircon. *Comm. Am. Ceram. Soc.*, **65** (1982) C-57–C-58.
12. Klug, H. P. & Alexander, L. E., Qualitative and quantitative analysis of crystalline powders. In *X-Ray Diffraction Procedure for Polycrystalline and Amorphous Materials*, 2nd edn. John Wiley and Sons, New York, USA, 1974, Chapter 7.
13. Wei, W., The quantitative XRD analysis of zircon/zirconia composite. Ceramics Process Systems Corp., Mass., USA, Internal Report, 1987.